

Distribution Agreement

In presenting this thesis as a partial fulfillment of the requirements for a degree from Emory University, I hereby grant to Emory University and its agents the non-exclusive license to archive, make accessible, and display my thesis in whole or in part in all forms of media, now or hereafter now, including display on the World Wide Web. I understand that I may select some access restrictions as part of the online submission of this thesis. I retain all ownership rights to the copyright of the thesis. I also retain the right to use in future works (such as articles or books) all or part of this thesis.

Ayjha Brown

April 10, 2024

The Mutational, Environmental and Immunological Drivers of Leukemia Resistance

By

Ayjha Brown

Dr. Christopher Porter

Advisor

Department of Chemistry

Dr. Christopher Porter

Advisor

Dr. Antonio Brathwaite

Committee Member

Dr. Miyoung Lee

Committee Member

Dr. Dailia Francis

Committee Member

2024

The Mutational, Environmental and Immunological Drivers of Leukemia Resistance

By

Ayjha Brown

Dr. Christopher Porter

Advisor

An abstract of

a thesis submitted to the Faculty of Emory College of Arts and Sciences of Emory University in

partial fulfillment

of the requirements of the degree of

Bachelor of Science with Honors

Department of Chemistry

2024

Abstract

The Mutational, Environmental and Immunological Drivers of Leukemia Resistance

By

Ayjha Brown

The therapeutic resistance of leukemia is shaped by mutational, environmental, and immunological drivers. Acute Lymphoblastic leukemia (ALL) is the most common malignancy in children and adolescents, accounting for 30% of all childhood cancers. B-cell Acute Lymphoblastic Leukemia (B-ALL) is the most common hematological malignancy found in children. Hematological neoplasms comprise a heterogeneous group of malignant disorders of the blood and bone marrow and are the most common childhood cancers. Deleterious alterations to DNA, also known as mutations, are the causative event behind these malignancies. In 2014, a patient presented with the first known case of leukemia harboring the SEPT9-ABL1 oncogenic fusion gene, showing resistance to tyrosine kinase inhibition. Obesity, which is a nationwide healthcare crisis, also contributes to survival outcomes in leukemia. Studies conducted by the Dr. Henry and Dr. Porter Laboratories have previously explored the relationship between the adipocyte microenvironment and the chemotherapy resistance in leukemia cells. There is data to suggest that since cancer cell phenotypes are distinct from cells of normal physiological function, they can initiate an innate immune response. Therefore, my work between the Dr. Henry and Dr. Porter Laboratories has entailed 1. exploring the impact of the SEPT9f-ABL1 mutation on leukemia oncogenicity and treatment responses, 2. studying the interplay between the adipocyte secretome and chemoresistance in leukemia and 3. investigating non-specific T-Cell killing mechanisms in

leukemia. *In Vitro* cell proliferation assays suggest that SEPT9f-ABL1 expression induces interleukin-3 independence in leukemia cell lines and correlates with downstream activation of pro-proliferative pathways. The simultaneous exploration of the adipocyte secretome from a single-cell transcriptomic as well as a proteomic standpoint revealed an adipocyte-induced increase in metabolic signatures associated with chemoresistance in both *in vitro* and in B-ALL patient samples. Lastly, T-cell killing Assays support cross-protective non-specific T-cell killing mechanisms in leukemia.

The Mutational, Environmental and Immunological Drivers of Leukemia Resistance

By

Ayjha Brown

Dr. Christopher Porter

Advisor

A thesis submitted to the Faculty of Emory College of Arts and Sciences of Emory University in
partial fulfillment

of the requirements of the degree of

Bachelor of Science with Honors

Department of Chemistry

2024

ACKNOWLEDGEMENTS

I would like to extend my sincerest gratitude to Dr. Christopher Porter. I have grown so much as a person and as a scientist under your mentorship. Thank you so much for affording me this opportunity. Thank you for always advocating for me.

I would also like to extend my warmest gratitude to Dr. Antonio Brathwaite, for your patient, unwavering support over the years. You have helped to shape me into the person that I am today. Thank you for always believing me, seeing the best in me and instilling confidence in me. You have been one of the strongest influences on my work ethic, drive, and character.

Thank you to Dr. Curtis Henry, for your amazing mentorship throughout my undergraduate career. You have always affirmed and uplifted me and continue to do so to this day. I am so grateful to have you as a mentor, and I hope to emulate your dedication and integrity when I eventually become a mentor for minority students like me.

Thank you to Dr. Miyoung Lee and Dr. Dailia Francis for your patience and guidance throughout my time in the lab. I deeply admire both of you as women in science, and I hope to mirror your skill, dedication, grace, and knowledge set and I navigate my own career.

Thank you to all the present and past members of the Dr. Henry and Dr. Porter Laboratories for fostering intellectual environments in which I could thrive. I extend utmost gratitude to MD candidate Kwame Armah, Uma Obalapuram, PhD candidate Delaney Geitgey, Dr. Jamie Hamilton, Mercy Coleman, Jodi Dougan and Kara Michaud.

Most of all, thank you to my family and friends for being my support system and safe place. To my parents, Natalie, and Brian, thank you for always cheering me on, and I hope that this makes you proud.

TABLE OF CONTENTS

SECTION I: How Does Mutation Impact Leukemia Cell Proliferation and Treatment

Responses?

Introduction.....	1
Materials and Methods	6
Results.....	9
Discussion And Future Directions.....	10

SECTION II: Environmental Drivers Of B-ALL

Introduction.....	12
Materials and Methods	14
Results.....	14
Discussion And Future Directions.....	16

SECTION III: Understanding Immunogenicity Towards B-ALL

Introduction.....	18
Materials and Methods	20
Results.....	22
Discussion And Future Directions.....	23

SECTION IV: FIGURES

Figure 1: The Structure of the Philadelphia Chromosome.....	24
Figure 2: IC-50 Curves for Imatinib, Dasatinib, Asciminib and Ponatinib in BaF3-MSCV-p190.....	25
Figure 3: Scheme for the Generation of SEPT9-ABL1 in pWPI Vector.....	26
Figure 4: The SEPT9f-ABL1 protein isoform is expressed,	

accompanied by downstream CRKL phosphorylation.....	27
Figure 5: SEPT9f-ABL1 expression induces IL-3 Independence in BaF3.....	28
Figure 6: High Fat High Sucrose Diet impairs normal B-cell function, reduces the frequency of B-cell populations, and downregulates gene programs associated with positive B-ALL outcomes in murine adipose tissue.....	29
Figure 7: The plasma of lean pediatric patients with B-ALL is exclusively characterized by the presence of heat shock proteins, cytoskeletal proteins, and proteins that promote cardiovascular health.....	30
Figure 8: Adipocytes secrete metabolites which may promote the growth of cancer cells.....	31
Figure 9: Adipocyte-secreted factors statistically significantly upregulate proteins associated with glutaminolysis, b-oxidation, B-progenitor cell development, and chemoresistance in the absence and presence of chemotherapy treatment.....	32
Figure 10: CD19 and CD95L Surface Ligand is stably expressed at high levels on B-ALL Cells.....	33
Figure 11: Jurkat T-Cells Recognize and Induce Apoptosis in Human B-ALL cells in a Non-Antigen Specific Manner.....	34
SECTION V: REFERENCES.....	35

SECTION I: How Does Mutation Impact Leukemia Cell Proliferation and Treatment

Responses?

Introduction

Leukemias comprise a heterogeneous group of malignant disorders of the blood and bone marrow(1). Deleterious alterations to DNA, also known as mutations, are the causative event behind these malignancies. They may result in the aberrant activation, suppression, and/or deletion of multiple types of proteins including growth factors, growth factor receptors, signal transducers, transcription factors, and programmed cell death regulators(2). These detrimental modifications manifest as the hallmarks of cancer: sustaining proliferative signaling, evading growth suppressors, avoiding immune destruction, enabling replicative immortality, tumor-promoting inflammation, activating invasion and metastasis, angiogenesis, genomic instability, evasion of apoptosis, and dysregulated cellular metabolism(3). As the field progresses, emerging hallmarks include phenotypic plasticity, non-mutational epigenetic reprogramming, polymorphic microbiomes, and senescent cells(4). Understanding these mechanisms is crucial for expanding our arsenal of treatment options as we improve the depth and durability of patient responses. Oncogenic fusion genes have made an impact on the treatment landscape of hematological malignancies. Among the most extensively characterized fusion genes is BCR-ABL1, also known as the Philadelphia chromosome (Ph). The Philadelphia chromosome is causative of most cases of chronic myeloid leukemia (CML), and 20-30% of acute lymphoblastic leukemia (ALL). This is the result of a translocation between the ABL1 gene on chromosome 9 and the BCR gene on chromosome 22 (**Figure 1**). ABL1 is a known protooncogene that encodes a protein tyrosine kinase. In response to growth factors, cytokines, cell adhesion, DNA damage, oxidative stress, and other signals, activated ABL induces cell proliferation, differentiation, survival, death,

retraction, or migration(4). It is ubiquitously expressed across all cells and tissues and is therefore considered essential. Therefore, tight regulation of ABL activity is necessary for normal cellular function. In contrast, BCR is thought to be a tumor suppressor gene whose product remains poorly understood. However, the molecular consequence of this sporadic event is a constitutionally active chimeric tyrosine kinase which retains the kinase domain from ABL-1. The BCR-ABL1 protein kinase initiates a complex signaling cascade resulting in abnormal cellular adhesion, aberrant cell proliferation, and anti-apoptotic mechanisms. Three chimeric BCR-ABL1 proteins of different molecular weights can be produced, namely p190, p210, and p230 (6). The p210 isoform is the hallmark of CML and is only expressed in about 25% of Ph-positive ALL. On the other hand, the p190 isoform is expressed in about 75% of Ph-positive ALL, and only 1-2% of CML. The p190 isoform is associated with additional cytogenetic abnormalities and poorer treatment responses(7,8).

Among the substrates of the BCR-ABL1 signaling cascade is the family of CRK and CRK-like (CRKL) proteins which are essential convergence points in tyrosine kinase signaling. CRKL-1, a key adaptor protein in the BCR-ABL1 signaling cascade, has historically been of great interest. Adaptor proteins facilitate the efficient positioning of other molecules in a signal transduction pathway, and are characterized by binding domains, binding motifs, and great structural flexibility. CRKL-1 contributes to fibroblast transformation by BCR-ABL to promote invasion, migration, angiogenesis, and immunosuppression, creating dynamic plasticity and facilitating treatment resistance and cancer progression(5). Since BCR-ABL1 induces phosphorylation and activation of CRKL-1, a high ratio of phosphorylated CRKL-1 (pCRKL-1) to CRKL-1 is indicative of high BCR-ABL1 activity and treatment resistance(9).

The primary goals of CML treatment can be stratified as follows: hematologic remission (normal complete blood cell count and physical examination), cytogenic remission (the elimination of Ph-positive cells), and molecular remission (the elimination of BCR-ABL1 transcripts)(10).

Standard chemotherapy, including alkylating agents (busulfan) and antimetabolites (hydroxycarbamide), have achieved hematological responses, but their lack of specificity resulted in minimal cytogenic or molecular remission(11). While allogenic stem cell transplantation in conjunction with aggressive chemotherapy regimens were shown to be curative during the 1980s, this procedure presents the risk of morbidity and mortality(12). Since older patients may present more risk for these complications, alternative treatments needed to be explored. With the mid 1980s came the advent of interferon alpha as a standard of care for CML, achieving both hematological and cytogenic responses. Interferon alpha is a cytokine therapy which “removes the brakes” of our immune system to improve anti-tumor responses(13).

However, between the years 1986 and 2000, the 5-year-survival of CML patients only increased from 29.72% to 46.16%(14).

Janet Rowley’s pivotal discovery of the Philadelphia chromosome in 1979 not only paved the way for the diagnosis and monitoring of hematological malignancies but for the development of efficacious targeted therapeutics. With 2001 came the approval of imatinib, which is the initiated the first generation of tyrosine kinase inhibitors (TKI) BCR-ABL1 to be FDA-approved for CML. Despite modest preclinical studies, clinical trials revealed unprecedented rates of complete cytogenic response revealed a level of efficacy that revolutionized the treatment landscape. Rates of complete cytogenic response were up to 40% in patients who previously failed interferon-alpha treatment, and up to 80% in patients with new diagnoses(15). After gaining traction for its efficacy in CML treatment, imatinib segued into treatment protocols for the Ph+ ALL(16).

However, molecular remission remained a significant challenge, as did the accumulation of point mutations and subsequent treatment resistance.

Imatinib's drawbacks eventually led to the discovery of dasatinib, which received FDA approval for CML and Ph-positive ALL in 2006, marking the advent of the second generation of TKI.

Dasatinib retained activity in the presence of most imatinib-resistant point mutations in BCR-ABL1. This may be attributed to fewer interactions with the P-loop, activation loop, and alpha helix of the BCR-ABL1 kinase domain. Another factor contributing to the potency of dasatinib is its ability to inhibit multiple protein kinases, including the SRC family kinases, receptor tyrosine kinases, and TEC family kinases, many of which are downstream targets of BCR-ABL1 (17).

However, both dasatinib and imatinib fail to address the T315I mutation, located at the so-called gatekeeper residue which forms a key H-bond interaction with both first and second-generation TKI(18).

The third generation of TKI was marked by the FDA approval of ponatinib, which was approved for second-line treatment of CML and Ph-positive ALL in the USA in 2012. A key structural feature of ponatinib is its unique carbon-carbon triple bond linkage that allows it to form interactions with the ATP binding pocket, even in the presence of the T315I mutation(19).

Allosteric inhibition has also been incorporated to circumvent the issue of ATP-binding pocket mutations. Asciminib is a potent, first-in-class inhibitor of BCR-ABL1 that Specifically Targets the ABL Myristoyl Pocket (STAMP)(66). It was approved in 2021 for patients presenting with Ph-positive ALL and CML. The constitutive activity of the BCR-ABL1 kinase is the loss of the regulatory myristoylated N-terminus of normal ABL, which binds to the myristoyl pocket of the kinase domain and regulates activity. However, asciminib replaces the function of this myristoylated N-terminus by directly binding to the myristoyl pocket and inducing inhibitory

conformational changes in BCR-ABL1(20). Asciminib is now used as a third-line and beyond treatment option for CML and Ph-positive ALL, and/or as another TKI option for patients presenting with the T315I mutation.

T-Cell Pro-Lymphocytic Leukemia, also known as T-PLL, is a very rare neoplasm, affecting approximately two (2) in one (1) million people each year. Presenting predominantly in patients over the age of 65, T-PLL is characterized by poor prognosis and minimal response to traditional chemotherapy and systemic monoclonal antibody treatment. Despite the curative implications of stem cell transplantation, this treatment strategy is not usually a viable option for older patients. As of 2023, T-PLL had median survival of only 3 years. Owing to its rarity, the mutational landscape of T-PLL is not extensively characterized, making targeted therapy a challenging endeavor(21).

In 2014, a patient presented with the first known case of T-PLL harboring the SEPT9-ABL1 fusion gene, showing resistance to imatinib and dasatinib(22). SEPT9 belongs to a family of cytoskeleton-associated genes called septins that are involved in a plethora of cellular functions including chromosome segregation, DNA repair, migration, and apoptosis. Overexpression of septins in multiple cancers has been extensively documented, and SEPT9 is now accepted as a biomarker for the early detection of colorectal cancer(23). However, the structure and function of SEPT9-ABL1 is largely misunderstood. Upon functional analysis of the SEPT9-ABL1 fusion, six isoforms were detected in the patient sample. Interleukin-3 (IL-3) is a multipotent hematopoietic growth factor, and IL-3 independent growth in hematopoietic cell lines is indicative of oncogenicity(24). Hematopoietic cell lines expressing the SEPT9f-ABL1 isoform showed the highest IL-3 independent proliferative capacity relative to other isoforms *in vitro*. Furthermore, cell lines expressing the SEPT9f-ABL1 isoform demonstrated resistance to

imatinib and dasatinib (reference). However, the response of SEPT9-ABL1 to third generation TKIs were not tested at the time of that report. Translational research can influence treatment protocols in the clinic. A local patient was recently found to harbor the SEPT9-ABL1 fusion protein in the leukemia and was denied TKI owing to existing literature suggesting that there would be no benefit. My project, spanning August 2023 to May 2024, aimed to test the hypothesis that SEPT9f-ABL1 is more responsive to new generation TKIs ponatinib and asciminib, than older generation TKIs dasatinib and imatinib(8,25), providing additional treatment options for patients with SEPT9f-ABL1+ leukemia.

Materials and Methods

BaF3 cell lines

Murine cell lines BaF3-MSCV-IRES-*GFP* (MIG), BaF3-MIG-p190, and parental BaF3 were gifted from the Dr. Graham and Dr. Porter laboratories (Department of Pediatrics at Emory University School of Medicine). All cell lines were cultured in WEHI conditioned media (WCM) consisting of RPMI1640 media (cat# 10-040-CV, Corning) supplemented with 10% heat-inactivated fetal bovine serum (FBS, cat# S11550, Atlanta Biologicals) and 10% WEHI-3B conditioned media with 1X Pen/Strep in a 37°C incubator. WEHI-3B cells were originally purchased from ATCC. RPMI 10% used for cell proliferation assays was comprised of RPMI1640 media (cat# 10-040-CV, Corning) supplemented with 10% heat-inactivated fetal bovine serum (FBS, cat# S11550, Atlanta Biologicals) and 1X Pen/Strep.

Plasmids and Retroviral Transduction

The pWPI-SEPT9f-ABL1 and pWPI vector control plasmids were generated by the Emory Integrated Genomics Core (EIGC) (RRID:SCR_023529). pSG5-ABL was a gift from Nora

Heisterkamp (Addgene plasmid # 31284 ; <http://n2t.net/addgene:31284> ; RRID:Addgene_31284). 293T cell line (originally from ATCC) was used for lentivirus production according to the Promega FuGENE® 6 Transfection Reagent Protocol (cat# E2691), conducted by Dr. Miyoung Lee. BaF3 parental cells were transfected with pWPI-SEPT9f-ABL1, pWPI-BCR-ABL1 and pWPI empty vector according to the Promega ViaFect™ Transfection Reagent (cat# E4981, Promega) protocol by Dr. Miyoung Lee. GFP+ cells were sorted by Dr. Miyoung Lee and seeded in RPMI10% for selection of IL-3 independent clones. **(Figure 3)**

Trypan Blue Exclusion Cell Proliferation Assays

To evaluate IL-3 independent cell proliferation, BaF3-MIG-p190, both clones of BaF3-pWPI-SEPT9f-ABL1, and pWPI-vector control were cultured in WCM and RPMI10% in a pre-sterile 24-well tissue culture plate at a density of 3×10^4 cells per well in 500 μ L of media. Cells were incubated at 37°C for 72 hours. At 24-hour intervals, 10 μ L aliquots of cell culture media were combined with 10 μ L aliquots of trypan blue. Cell counts and viabilities were retrieved using the Cellometer K2 Cell Counter owned by both the Dr. Porter and Dr. Graham laboratories.

CellTiter 96® Non-Radioactive Cell Proliferation Assay

To establish IC-50 dose-response curves for imatinib, dasatinib, ponatinib, and asciminib (all purchased from Thermo Scientific™), BaF3-MSCV-p190 cells were seeded in a pre-sterile round bottom 96-well plate at a density of 5×10^5 cells per well in 10% RPMI1. Each drug treatment was completed in triplicate. DMSO served as a baseline control for treatment responses. Cell proliferation data was obtained via the Promega Standard CellTiter 96® Assay Protocol for 96-Well Plates (cat #G4000, Promega) after 72 hours of CO₂ incubation at 37°C for 72 hours. BioTek Gen5 software was used to analyze absorbance at 570 nm and 700 nm. **(Figure 2)**

Immunoblotting

To confirm the expression of BCR-ABL1, SEPT9f-ABL1, phosphorylated CRKL, and CRKL, pWPI-BaF3-SEPT9-ABL1, and pWPI-BaF3-BCR-ABL1 were cultured in WCM, and CO₂ incubated at 37°C until a concentration of 1x10⁶ cells per mL was achieved. Five mL aliquots of each cell line were collected, and protein was isolated in accordance with the Thermo Scientific™ RIPA buffer protocol (cat # 89901, Thermo Scientific™) for lysis and extraction of suspension-cultured mammalian cells. Whole lysate protein samples were quantified using Pierce™ Dilution-Free™ Rapid Gold BCA Protein Assay (cat# A55860, Thermo Scientific™) and the BioTek Gen5 software. Samples were resolved using Invitrogen Power Blotter Pre-cut Nitrocellulose Membranes and Filters (cat # PB7220, Thermo Scientific™). All primary and secondary antibodies were sourced from Cell Signaling Technology. SEPT9f-ABL1 and BCR-ABL1 were detected using cABL1 primary antibody (1:1000, cat #2862, 1:5000). Primary antibodies were also used to detect phospho-CRKL (1:5000, cat #3181), CRKL (1:5000, cat # 38710) and beta-actin (1:2000, cat #4970). Beta-actin served as a loading control. Secondary antibodies used for visualization were also used (1:5000) with the Li-Cor Odyssey CLx. (Figure 4)

CellTiter-Glo® Luminescent Cell Viability Assay

To determine the differential treatment responses of pWPI-SEPT9f-ABL1 and pWPI-BCR-ABL1 to TKI, stable pWPI-SEPT9f-ABL1 and pWPI-BCR-ABL1 cell lines were seeded in sterile 96 well plates with varying concentrations of dasatinib, ponatinib, asciminib. Metabolic activity was quantified in accordance with the CellTiter-Glo® Luminescent Cell Viability Assay (cat #G7570, Thermo Scientific™).

Results

SEPT9f-ABL1 expression induces IL-3 Independence in BaF3

To assess the IL-3 independence of pWPI-SEPT9f-ABL1 proliferation, cell counts per mL were plotted at 24, 48, and 72 hours respectively in the presence of IL-3 (WCM) and absence of IL-3 (10% RPMI; n=4 independent experiments), alongside pWPI-BCR-ABL1 (n=1), MSCV-p190 (n=3), and pWPI (vector control; n=4). Both clones of pWPI-SEPT9f-ABL1 demonstrated statistically significantly greater IL-3-independent proliferation relative to the vector control after 72 hours of incubation. While MSCV-p190 demonstrated elevated IL-3 independent proliferation relative to pWPI vector control, this was not statistically significant (p=0.05). In the absence of IL-3, there was not a statistically significant difference between any of the pWPI-SEPT9f-ABL1 clones and the vector control (p=NS). There was also no statistically significant difference between either of the pWPI-SEPT9f-ABL1 clones and MSCV-p190 in any condition tested (p=NS) (Figure 5).

SEPT9f-ABL1 Induces the Constitutive Phosphorylation of CRKL

The expression of the SEPT9f-ABL1 isoform was confirmed via western blot at a molecular weight at approximately 130 KDa in both clones of pWPI-SEPT9f-ABL1. The expression of BCR-ABL1-p190 isoform was similarly confirmed in pWPI-BCR-ABL1 at approximately 190 KDa. pWPI vector control showed no expression of SEPT9f-ABL1 or BCR-ABL1-p190. pWPI-BCR-ABL1, and both clones of pWPI-SEPT9f-ABL1 showed phosphorylation of CRKL at approximately 39 KDa. pWPI vector control showed no phosphorylation of CRKL. pWPI-BCR-ABL1, both clones of pWPI-SEPT9f-ABL1, and pWPI-vector control showed expression of both beta-actin (approximately 45KDa) and CRKL (approximately 39 KDa).

Sensitivity of SEPT9f-ABL1 cells to TKI

These experiments are underway, so there are no results to report to date.

Discussion

This study sought to further characterize the SEPT9f-ABL1 fusion protein, addressing a gap in knowledge surrounding this oncoprotein. The pWPI-SEPT9f-ABL1 and pWPI-BCR-ABL1 cell lines showed constitutive phosphorylation of CRKL. CRKL phosphorylation was absent in the control cell line. The constitutive phosphorylation of CRKL by SEPT9f-ABL1 demonstrates the activation of this pivotal signaling pathway, including phosphorylation of the PI3 kinase and subsequent oncogenicity via anti-apoptotic mechanisms(25). The statistically significant IL-3 independent proliferation of pWPI-SEPT9f-ABL1 relative to the vector control further establishes the oncogenicity of our pWPI-SEPT9f-ABL1 cell lines. To establish working concentrations of TKI to use in our functional analysis of SEPT9f-ABL1, we generated IC-50 curves in Graphpad Prism for pWPI-BCR-ABL1 using CellTiter 96® Non-Radioactive Cell Proliferation Assay. The IC-50 of ponatinib (0.58 nM), asciminib (16 nM), imatinib (602 nM) and dasatinib (0.11 nM) were extrapolated. Due to time constraints, we have challenged the SEPT9f-ABL1 cell lines with imatinib, dasatinib, asciminib, and ponatinib, only once, so no conclusions can be drawn at this time. However, a preliminary foundation has been set for the exploration of this project by the Porter Laboratory.

My immediate next steps would be additional replicates of the CellTiter-Glo® Luminescent Cell Viability Assay to quantify dose responses of SEPT9-ABL1 to TKI. Ideally, I would also assess for apoptosis by flow cytometry using Annexin V and propidium iodide. This would provide a comprehensive perspective of the dose-response from proliferation and cell death perspectives.

The BaF3-SEPT9f-ABL1+ cell lines could also be studied *in vivo* to elucidate differences in survival outcomes between the older and newer generations of TKI.

As of 2023, intravenous alemtuzumab and cytotoxic chemotherapy remain the treatment protocol for T-PLL. This regimen is considered palliative because of its lack of specificity, poor patient outcomes, and significant morbidity risk(26). The impact of the SEPT9f-ABL1 fusion gene in T-PLL is largely unelucidated owing to its rarity. T-PLL patients harboring the SEPT9f-ABL1 fusion gene may benefit from more targeted treatment outcomes and improved survival. Today, CML patients have life expectancies closely resembling normal healthy adults owing to the advent of targeted TKI. Screening for the SEPT9f-ABL1 fusion gene in other rare, aggressive malignancies may provide useful context for the incorporation of TKI into treatment regimens.

SECTION II: Environmental Drivers of B-ALL

Introduction

The obesity pandemic is a rapidly worsening crisis affecting approximately 50% of the adult population in the United States. By the year 2030, it is projected that nearly 1 in 4 adults will have severe obesity(27,28). A staggering 14.7 million American children and adolescents (aged 2-19 years) are impacted by obesity(27,28). Obesity as a key determinant of clinical outcomes in pathological settings has been extensively documented in the context of pathogenic infections(29), as well as cancer(30). A comprehensive understanding of the obese microenvironment is therefore imperative for the future of precision medicine.

The increased prevalence of obesity has led to the exploration of adipose tissue as an endocrine organ playing numerous systemic roles in metabolic diseases(38). Adipose tissue (AT) is located beneath the skin and adds insulation and mechanical protection to our internal organs.

Adipocytes are the cells that comprise adipose tissue. The diverse collection of molecules secreted by adipocytes is known as the secretome. While some studies have implicated obesity as a factor contributing to worsened cancer survivorship(35,36), there is data to suggest a positive correlation between cancer outcomes and longer survival in cancer patients(39). Thus, elucidating the impact of adipocyte secretome on expression profiles of leukemia is pivotal as we inform clinical decisions and improve patient outcomes.

B-cell Acute Lymphoblastic Leukemia (B-ALL) accounts for approximately 85% of ALL cases and is the most common hematological malignancy found in children(32). B-ALL is characterized by the aberrant proliferation and survival of B precursor-stage lymphoid cells within the bone marrow, blood, and extramedullary sites owing to deleterious mutations(32,33).

The consequence of these genetic alterations is the replacement of normal lymphoid progenitor cells with malignant cells, overriding normal hematopoiesis.

The pharmacokinetics of chemotherapy in obese patients has been extensively documented(35,36). Adipocytes have been demonstrated to attract and protect B-ALL cells from the effects of chemotherapy. Additionally, adipocyte secretome-mediated chemoresistance has been extensively illustrated in methotrexate (MTX), doxorubicin, daunorubicin, and vincristine(41-44). It has been shown that the aggressiveness of B-ALL in the obese microenvironment is partially fortified by the secretion of metabolites upon which malignant cells can rely. This allows them to circumvent the hurdle of limited metabolite resources, inducing pro-proliferative and anti-apoptotic phenotypes(45). Studies conducted by the Dr. Henry and Dr. Porter Laboratories have also explored the relationship between the adipocyte microenvironment and the genomic and phenotypic profiles of leukemia cells. Galectin-9, which is a protein secreted by adipocytes that supports cell adhesion, contributes to chemoresistance in B-ALL by the induction of cellular senescence(34). The ambitious study detailed herein simultaneously explored the adipocyte secretome profile from a single-cell transcriptomic as well as from a proteomic standpoint. This multi-omic approach has provided compelling evidence for the role of the adipocyte secretome in priming B-ALL cells for resistance against chemotherapy. Our data also implicates the adipocytes in the secretion of known oncogenic biomarkers, as well as the induced upregulation of expression profiles on non-malignant B-cells that are associated with poor survival outcomes and more aggressive disease.

Materials and Methods

All materials and methods including *Cell Lines, Human Samples, Murine adipose immune cell study, and adipose tissue fluorescence-activated cell sorting* are published by Geitgey, et. al.(27). *I directly contributed “Cell Lines” and “Fluorescence-Activated Cell Sorting”, as well as the review process of this publication.*

Results

High Fat High Sucrose Diet impairs normal B-cell function, reduces the frequency of B-cell populations, and downregulates gene programs associated with positive B-ALL outcomes in murine adipose tissue.

To test the hypothesis that the adipocyte microenvironment may impair the function or distribution of normal B cells, single-cell RNA-sequencing was performed on blood cells obtained from lean (low fat low sucrose diet) and obese mice (high fat, high sucrose diet). Obese mice showed a reduced population of non-malignant B-cells. Most notably, gene expression analysis of non-malignant B-cells from lean mice showed high expression of gene associated with the regulation of B-cell transformation, the suppression of aberrant B-cell activation and the control of apoptosis in lymphocytes. Further analysis revealed that pathways implicated in lymphocyte activation, leukocyte activation, immune response related signaling and B-cell receptor activation are upregulated in non-malignant B-cells from lean mice relative to obese mice. To add clinical context to these findings, Therapeutically Applicable Research to Generate Effective Treatments (TARGET)-ALL-P2-B-cell dataset was mined to explore possible correlations between these observed expression profiles and survival outcomes. Surprisingly, the

upregulated gene signatures in non-malignant B-cells from lean mice conferred a statistically significant survival advantage in B-ALL patients (**Figure 6**).

Changes in circulating factors are associated with obesity in nonleukemic donors and patients with B-ALL.

After exploring the impact of the adipocyte secretome on the expression non-malignant B cells, we explored the circulating systemic factors in nonleukemic human donors to provide insight into the molecular drivers behind these expression profiles. Strikingly, phospholipid transfer protein and histidine-rich glycoprotein were upregulated in sera from lean donors in comparison to obese donors. The deregulation of phospholipid transfer protein has been implicated in atherosclerosis, while histidine glycoprotein is a multifunctional adaptor molecule that regulates immunity, pathogen clearance, coagulation, and angiogenesis(45-47). Additionally, CDL5, which is a marker for inflammation(48), was detected at elevated levels in sera from obese nonleukemic donors relative to lean non-leukemic donors. Upon analysis of pediatric B-ALL patients, it was found that immunoglobulin proteins, heat shock associated proteins, cytoskeleton-associated proteins, signatures associated with B-cell activation and hemoglobin-associated proteins were upregulated in the sera of obese pediatric B-ALL patients. (**Figure 7**)

The adipocyte secretome contains metabolites that promote oncogenic proliferation and alter the metabolic state of human B-ALL cells in the presence and absence of MTX.

After profiling the sera and plasma human samples in adipocyte-rich microenvironments, *in vitro* assays were utilized to directly examine and isolate the adipocyte secretome. It was found that numerous metabolites were upregulated in B-ALL cell lines in the presence of adipocyte conditioned media (ACM) relative to bone marrow stromal cell conditioned media (SCM) and unconditioned media (UCM). Most notably, aspartate and hydroxyanthranilic acid were

upregulated in ACM, which provide proliferative advantages for leukemia cells by via hypoxic survival mechanisms and immune evasion respectively(49,50). These trends in metabolic activity were largely conserved upon challenging cell lines with MTX.

ACM induced increased glutaminolysis, b-oxidation, and glutathione metabolism relative to UCM and SCM. Strikingly, the only protein that was downregulated by ACM in both the absence and presence of MTX was AMTOR, a biomarker whose downregulation implicated in slow tumor proliferation and subsequent resistance to chemotherapy, which specifically targets rapidly proliferating cells(51) (**Figure 8-9**).

Discussion

The multi-omics analysis of the adipocyte secretome has provided pivotal insight into the mechanisms of B-ALL progression and chemoresistance. Adipose tissue hypoxia is currently being explored as a driving factor behind adipose tissue dysfunction, including chronic inflammation and altered metabolic responses(52). The induction of hypoxic signatures by the adipocyte secretome is supported by our data. Higher expression levels of the pro-angiogenic histidine glycoprotein were detected in sera from lean non-leukemic patients, relative to obese non-leukemic patients. Additionally, heightened levels of hemoglobin-associated proteins were detected in sera from lean pediatric B-ALL patients relative to obese pediatric B-ALL patients. These observations are accompanied by the synergistic increase in adipocyte secretion of metabolites such as aspartate, which confer a survival advantage under hypoxic conditions(53). Future projects could examine the response of B-ALL in ACM with the synergistic combination of hypoxia-inducible factor inhibition and MTX.

The dawn of cancer immunotherapy has also provided new avenues for B-ALL treatment with curative implications. The Dr. Henry and Dr. Porter Laboratories have extensively characterized the impact of dampened T-cell function on the modulation of anti-cancer mechanisms(53). The secretion of agents that are known to be cytotoxic to T-cells supports these findings and may contribute to the relative inefficacy of bispecific T-cell engagers, such as blinatumomab, in adipocyte rich microenvironments. Monoclonal antibody treatment is currently being explored to restrict the activity of oncogenic obesity-induced factors, such as Siglec-15. Siglec-15 antibody treatment may be used synergistically with bi-specific T-cell engagers to potentially improve patient responses(54). Recent studies also suggest that the T-cell exhaustion phenotype may confer heightened responses to anti-PD-1 and anti PD-L1 immunotherapy, thereby opening avenues for even more synergistic applications(55). Additionally, the relationship between aneuploidy and cytoskeletal protein dysregulation could be further explored to elucidate the key mechanisms behind this immunogenicity(56).

SECTION III: Understanding Immunogenicity Towards B-ALL

Introduction

The immune system plays a pivotal role in identifying and eradicating oncogenic cells. The immune response is a highly conserved defensive three-fold mechanism: recognition, processing, and reaction(57). Cells, or active molecules involved in this process, recognize non-self-elements that enter our bodies. Natural killer (NK) cells, macrophages, dendritic cells (DC) and neutrophils all participate in the innate immunity process. When cells implicated in innate immunity mechanisms encounter pathogenic elements, a highly specific recognition process is triggered, which results in subsequent elimination of the element via phagocytosis, inflammatory responses in the form of cytokine production, or opsonization via the complement system (58). While innate immunity relies on pattern recognition of non-self-antigens, adaptive immunity relies on the recognition of specific “non-self” antigens for the development of pathogen-specific immunological responses and immunological memory(59). Adaptive immunity is largely regulated by CD4+ and CD8+ T-lymphocytes, as well as B-lymphocytes.

Cancer cells may express surface antigens that can be recognized by both the innate and adaptive immune system’s surveillance mechanisms. In ideal situations, cells that possess genetic abnormalities express phenotypes making them distinct from cells of normal physiological function. CD8+ T-lymphocytes have been implicated as effectors at the intersection of adaptive and innate immunity, and the success of many cancer immunotherapies is quantified by their ability to mount a tumor-specific CD8+ T-lymphocytic response (59). However, as referenced in Section I, avoiding immune destruction is one of the hallmarks of cancer (4). Unfortunately, despite their genetic abnormalities, malignant cells often closely resemble our normal cells and are thereby able to circumvent or silence our surveillance mechanisms, leading to aberrant

proliferation and tumorigenesis. Therefore, the mechanisms via which cancer cells evade the immune system are an area of great interest in today's cancer treatment landscape.

As extensively discussed in Section II, obesity is an ongoing health crisis(27,28) Chronic inflammation, which is a byproduct of adiposity, is strongly correlated with the development of malignancy(57). Oxidative stress and tissue damage are well-documented characteristics of high adipose environments(58). Chronic inflammation may lead to exhausted T-cell phenotypes and dampened immunosurveillance. As previously mentioned, multiple metabolites present in the adipocyte secretome act synergistically with these induced hypoxic conditions to encourage oncogenic proliferation and subsequent aggressiveness in the case of B-ALL(27). Therefore, elucidating T-lymphocyte killing mechanisms in adipocyte-rich contexts is of great relevance. The Hygiene Hypothesis was first posited by David P. Strachan in 1989 after noticing a greater incidence of hay fever and asthma among smaller households relative to larger households(59). This observation eventually evolved to the proposition that a lack of pathogenic exposure in childhood leads to immune dysregulation and chronic inflammation. A study detailing the incidence of acute lymphoblastic leukemia (ALL) showed that social contact in early life (daycare attendance prior to 6 months old or having an older sibling) was potentially protective and associated with reduced ALL risk(60). This implies that immune function is enhanced by antigenic exposure, and that this development may be cross protective against hematological neoplasms.

To investigate non-specific T-lymphocyte killing mechanisms, we looked to the CD95/CD95L pathway. Long considered a death receptor/death ligand system, this interaction was thought to be key for the eradication of cancer cells. Recent data suggests that the CD95/CD95L targeted therapies may be ineffective owing to the side effects of systemic treatment, and the resistance of

many cancer types to CD95/CD95L inhibition(61). However, the role CD95/CD95L pathway in immune evasion in B-ALL remains largely understood. We hypothesized that vaccinations against pathogens produce memory T-cells capable of non-specific cross protection against the development of B-ALL via the CD95/CD95L pathway. To test this hypothesis, we will use a combination of *in vitro* assays including to quantify T-cell mediated cytotoxicity and CD95/CD95L expression in B-ALL.

Materials and Methods

The materials and methods included herein were completed in conjunction with Kwame Armah(67).

Cell Lines

As previously described and published by the Henry Laboratory , human B-ALL cell lines were a generous gift from the Dr. Graham and Dr. Porter Laboratories (Department of Pediatrics at Emory School of Medicine)(34). Nalm6 cell lines were cultured in RPMI1640 (cat# 10-040-CV corning) supplemented with 10% fetal bovine serum (FBS, cat# S11550 Atlanta Biologicals) (34). REH, SEM, RCH-AcV cell lines were grown in RPMI1640 supplemented with 20% FBS. OP-9 bone marrow stromal cells were grown in Alpha-Minimum Essential Medium (α MEM, cat# 15-012-CV, Corning) supplemented with 20% FBS(34).

Flow Cytometry Analysis of CD95L Surface Stains

To elucidate the surface expression of CD95 and CD95L, we plated 82% viable RCH-ACV cells at a concentration of 2.5×10^5 cells/mL in three different media conditions and followed by CO₂ incubation for 48 hours: Adipocyte Conditioned Media (ACM), Stromal Conditioned Media (SCM), and RPIMI1640 media supplemented with 10% FBS (UCM). After 48 hours, the cells

were replated in a 96 well plate in triplicates, at a density of 10^5 cells per well. Each well, except for the unstained and isotype control, was treated with 1:100 dilution of CD95L fluorescent antibodies and subjected to 1 hour incubation. The surface expression CD95-L was then quantified via flow cytometry.

T-Cell Mediated Cytotoxicity Assay with Co-culture Experiments

Jurkat T-cells were plated at a concentration of 2×10^6 cells per well in UCM in a 12-well plate. One well was stimulated with a phorbol 12- myristate 13-acetate (PMA) and ionomycin cocktail (high, medium, and low stimulated groups), while the control well was left unstimulated. Human B-ALL cell lines were labeled with cell tracker orange and cell trace yellow and incubated in UCM for 24 hours after 48 hours of Jurkat T-cell stimulation. After 72 hours, Jurkat T cells were split into four groups: ACM stimulated and labeled with cell tracker orange, UCM stimulated and labeled with cell tracker orange, SCM stimulated and labeled with cell tracker orange, and unstimulated and labeled with cell tracker orange. Human B-ALL cells were then plated at 5.0×10^4 cells/well in 96-well flat bottom plate. Jurkat T-cells were then added at 2:1 Jurkat T:B-ALL cells (10^5 cells/well); 1:1 Jurkat T:B-ALL cells (5.0×10^4 cells/well); 1:2 Jurkat T:B-ALL cells (2.5×10^4 cells/well). T-cells were plated in a volume of 100 μ l of media/well and B-ALL cells were added at 100 μ l of media/well. To observe biological B-ALL activity in the absence of T-lymphocytes, human B-ALL cells were also plated alone at 10^4 cells per well. Unlabeled cells served as a negative control. The plate was then analyzed by flow cytometry using the Cytoflex to detect T-Lymphocyte mediated killing mechanisms.

Adipocyte Differentiation Protocol

Previously documented and published by the Henry Laboratory(34).

Results

The results included herein were completed in conjunction with Kwame Armah(67).

CD19 and CD95L Surface Ligand is stably expressed at high levels on B-ALL Cells

CD19 belongs to the immunoglobulin superfamily and is considered a B-lymphocyte marker (62). The percentage of B-ALL cells expressing CD19 were detected based on treatment groups: UCM (n=5, 79.43%), SCM (n=5, 76.33%) and ACM (n=5, 77.16%). Similarly, the percentage of B-ALL cells expressing CD19 were detected based on treatment groups: UCM (n=5, 54.9%), SCM (n=5, 54.26%), and ACM (n=5, 62.93%). There was no significant difference in expression of CD19 and CD45 among treatment groups. There was also no significant difference between maximum fluorescent intensity of either CD19 or CD95L across growth conditions (**Figure 10**).

Jurkat T-Cells Recognize and Induce Apoptosis in Human B-ALL cells in a Non-Antigen Specific Manner

In the absence of Jurkat T-cells, B-ALL were 89% viable, experiencing only 11% spontaneous cell death according to cell trace yellow staining. The level of PMA/ionomycin did not impact the degree of T-cell-mediated killing, regardless of the ratio of Jurkat T-cells to B-ALL. In the presence of stimulated Jurkat T-cells, B-ALL cells experienced spontaneous cell death of up to 34.7% (**Figures 11**). This data, coupled with the fact that Jurkat T-cells had never encountered B-ALL supports the hypothesis of anti-cancer immunity via T-cell-mediated cross-protection.

Discussion

Considering our discussion of tyrosine kinase inhibition in Section I and chemotherapy in Section II, evaluating the intrinsic immunogenicity of B-ALL provides necessary context to frame our understanding of leukemia progression. The high expression of CD19 on the surface of B-ALL has paved the way for bispecific anti-CD19 CAR T cells for relapsed, refractory B cell malignancies(62). As previously mentioned, the adipocyte secretome may reduce the efficacy of CAR T cell therapy owing to an induced T-cell exhaustion phenotype(63). While this study did not explore the impact of obesity on non-specific T-cell killing efficacy, further experiments could be completed to determine whether this trend also extends to non-specific T-cell killing mechanisms. Other markers of T-cell exhaustion, such as SLAMF7 could also be explored in the context of T-cell killing mechanisms in adipocyte-rich environments(65).

Additionally, it was also previously mentioned that anti-PD-1/PD-L1 immune checkpoint blockade therapy (pembrolizumab) may invigorate T-cells with exhaustion phenotype, and possibly enhance the efficacy of immune checkpoint blockade(64). Further T-cell killing assays could also be completed to elucidate the effect of the adipocyte secretome on the efficacy of immune checkpoint blockade. Despite the demonstrated lack of efficacy of anti-CD95/CD95L therapeutics, conducting T-Cell killing assays in adipocyte-conditioned media accompanied by CD95/CD95L blockade could reveal a synergistic or antagonistic relationship between the adipocyte secretome and the CD95/CD95L interaction.

SECTION IV: Figures

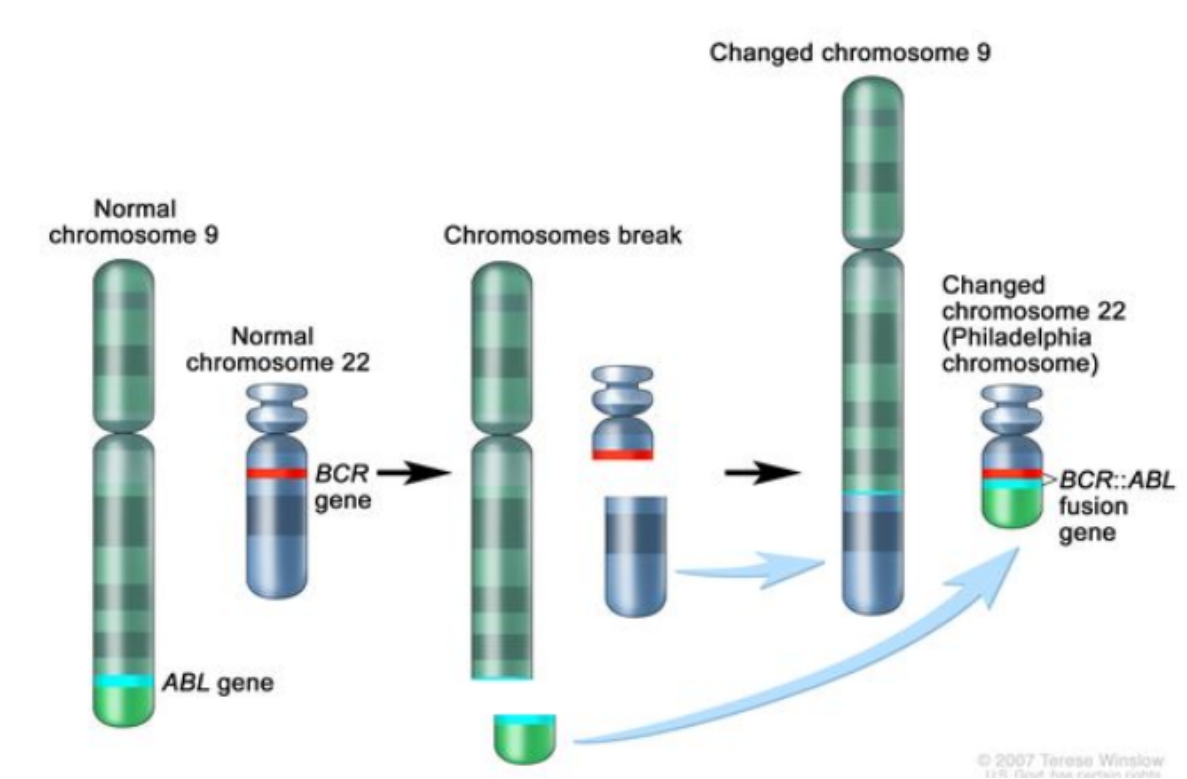


Figure 1: The Structure of the Philadelphia Chromosome

Adapted from: Sholikhah, Tri. (2017). Fusion gene bcr-abl: From etiopathogenesis to the management of chronic myeloid leukemia. *Jurnal Kedokteran dan Kesehatan Indonesia*. 8. 29-37.

10.20885/JKKI.Vol8.Iss1.art5.

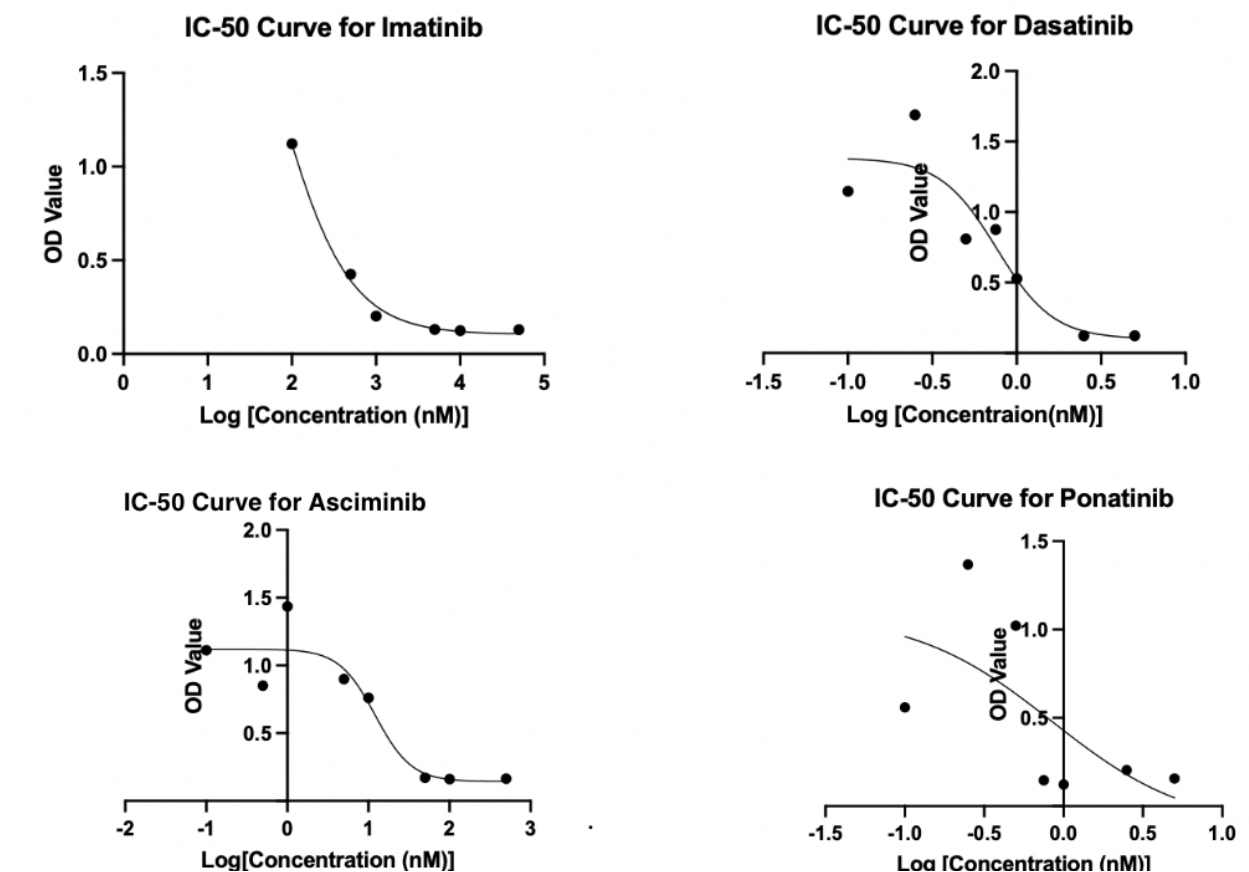


Figure 2: Dose response Curves for Imatinib, Dasatinib, Asciminib and Ponatinib in BaF3-MSCV-p190. BaF3-MSCV-p190 cells were seeded in a pre-sterile round bottom 96-well plate at a density of 5×10^5 cells per well in 10% RPMI1. Each drug treatment was completed in triplicate. DMSO served as a baseline control for treatment responses. Cell proliferation data evaluated via the Promega Standard CellTiter 96® Assay Protocol for 96-Well Plates (cat #G4000, Promega) after 72 hours of CO₂ incubation at 37°C for 72 hours. BioTek Gen5 software was used to analyze absorbance at 570 nm and 700 nm.

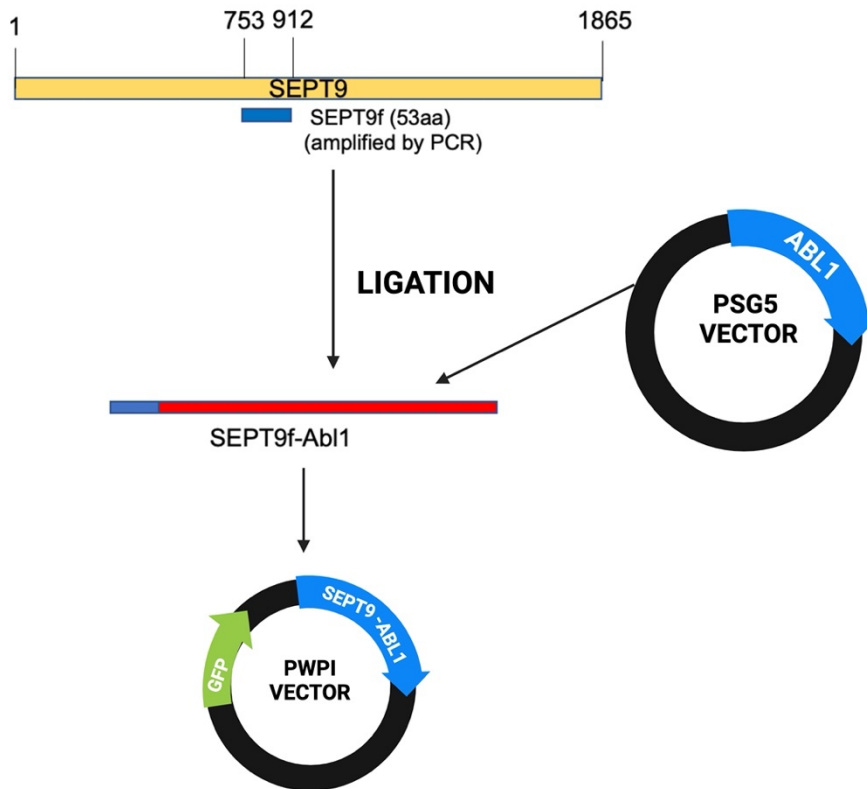


Figure 3: Scheme for the Generation of SEPT9-ABL1 in pWPI Vector.

Created with BioRender.

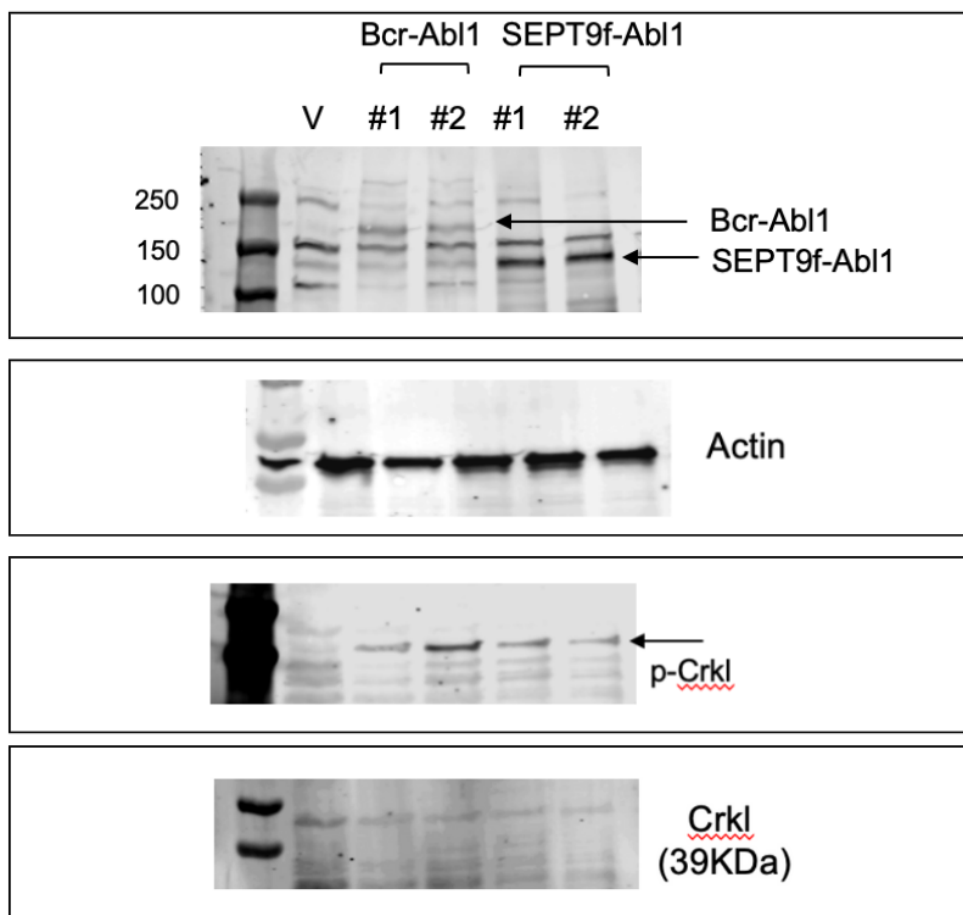


Figure 4: The SEPT9f-ABL1 protein isoform is expressed, accompanied by downstream CRKL phosphorylation. SEPT9f-ABL1 and BCR-ABL1 were detected using cABL1 primary antibody. Primary antibodies were also used to detect phosphorylated-CRKL, CRKL (1:5000, cat # 38710) and beta-actin (1:2000, cat #4970). Beta-actin served as a loading control.

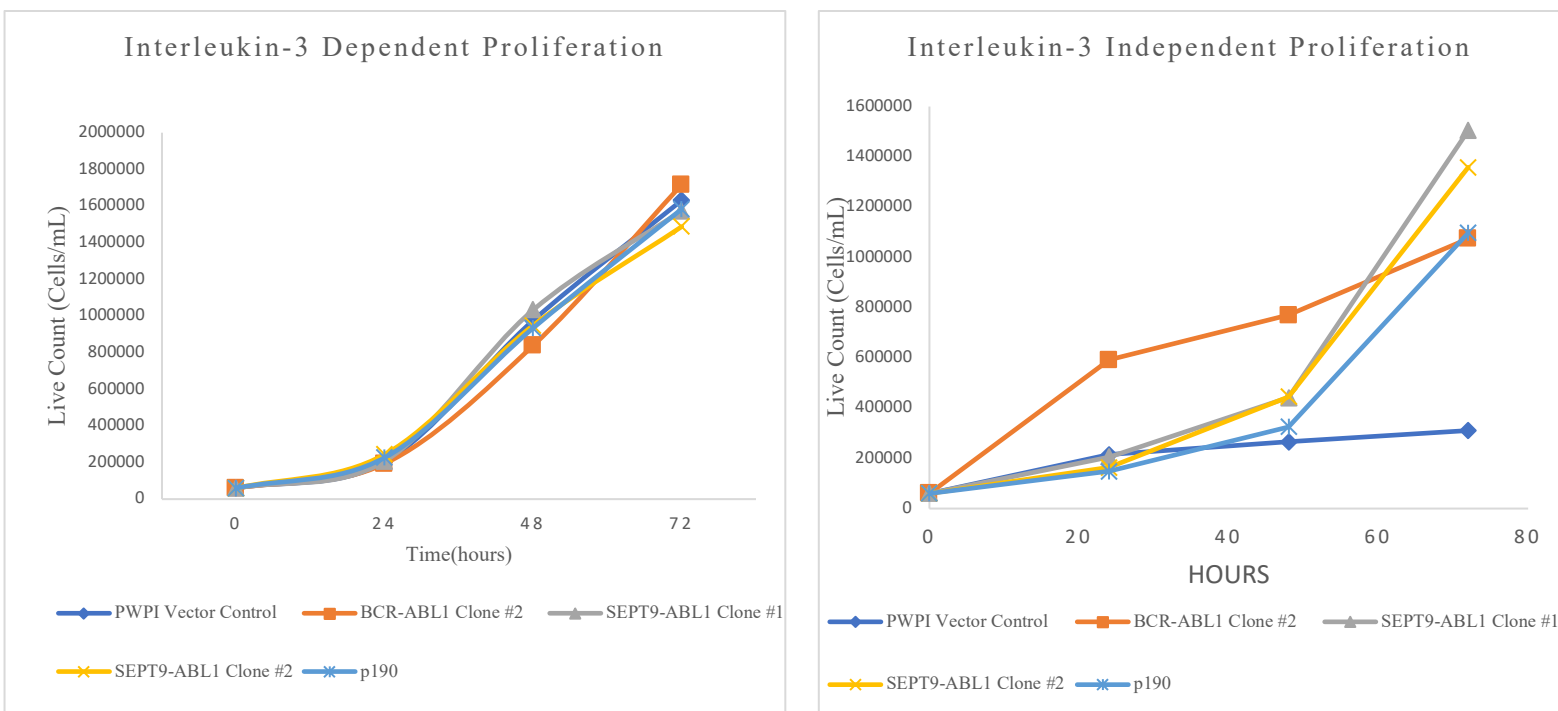


Figure 5: SEPT9f-ABL1 expression induces IL-3 Independence in BaF3. BaF3-MSCV-p190, BaF3-pWPI-SEPT9f-ABL1, and pWPI-vector control were cultured in WCM and RPMI10% in a pre-sterile 24-well tissue culture plate at a density of 3×10^4 cells per well and CO_2 incubated at 37° . At 24-hour intervals, cell counts per mL were retrieved via trypan blue exclusion assay and plotted at 24, 48, and 72 hours respectively in the presence of IL-3 (WCM) and absence of IL-3 (10% RPMI) (n=4 independent experiments), alongside pWPI-BCR-ABL1 (n=1), MSCV-p190 (n=3), and pWPI (vector control; n=4). pWPI-SEPT9f-ABL1 demonstrated statistically significantly greater IL-3-independent proliferation relative to the vector control after 72 hours of incubation ($p < 0.05$). While MSCV-p190 demonstrated elevated IL-3 independent proliferation relative to pWPI vector control, this was not statistically significant ($p = 0.05$). In the absence of IL-3, there was no statistically significant difference between any of the pWPI-SEPT9f-ABL1 clones and the vector control ($p = \text{NS}$). There no statistically significant difference between pWPI-SEPT9f-ABL1 and MSCV-p190 in any condition tested ($p = \text{NS}$).

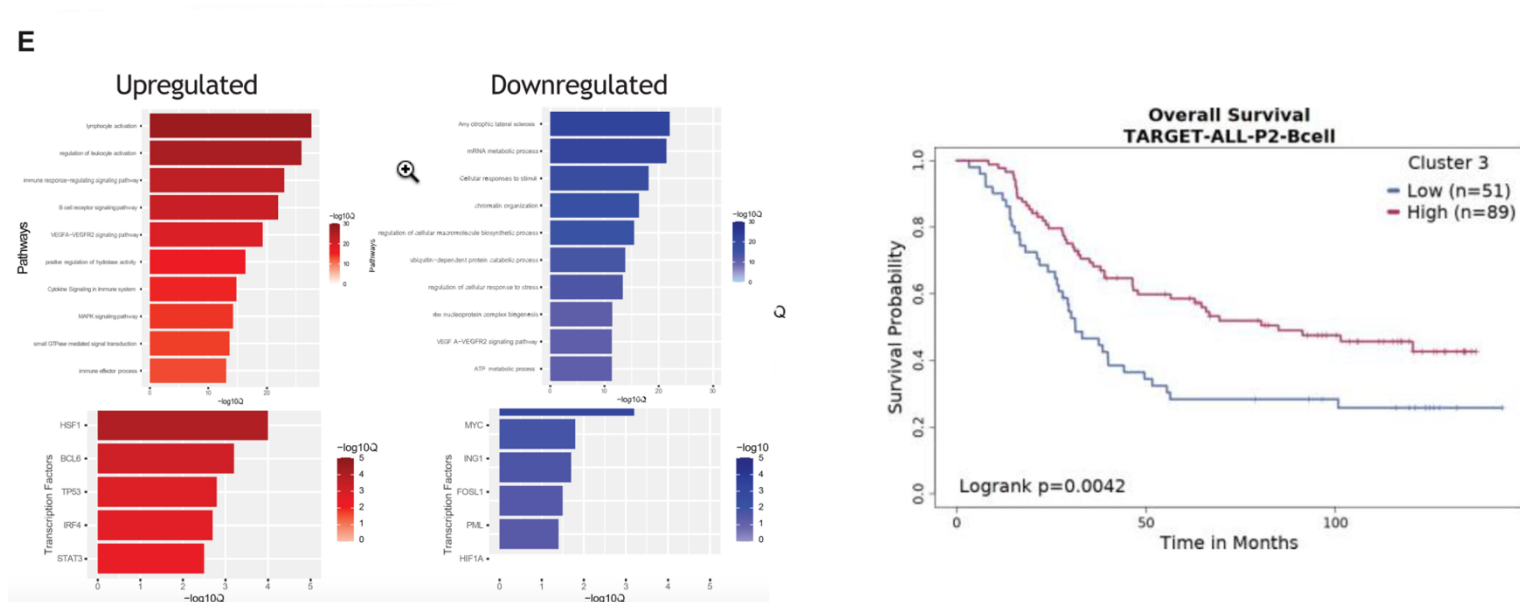


Figure 6: “High Fat High Sucrose Diet impairs normal B-cell function, reduces the frequency of B-cell populations, and downregulates gene programs associated with positive B-ALL outcomes in murine adipose tissue. E) Statistically significantly upregulated (red) and downregulated (blue) pathways/GO and transcriptional factors in lean mice F) Overall survival probability plot for the expression of top 10 upregulated genes in lean mice) in the TARGET-ALL-P2-B- cell dataset using the survival genie platform. Statistical significance in Figure 1, B, as determined by the student t test, is denoted by ** P < .0001. B-ALL = B-cell acute lymphoblastic leukemia; UMAP = uniform manifold approximation and projection.”**

Citation: Geitgey DK, Lee M, Cottrill KA, Jaffe M, Pilcher W, Bhasin S, Randall J, Ross AJ, Salemi M, Castillo-Castrejon M, Kilgore MB, Brown AC, Boss JM, Johnston R, Fitzpatrick AM, Kemp ML, English R, Weaver E, Bagchi P, Walsh R, Scharer CD, Bhasin M, Chandler JD, Haynes KA, Wellberg EA, Henry CJ. The 'omics of obesity in B-cell acute lymphoblastic leukemia. *J Natl Cancer Inst Monogr.* 2023 May 4;2023(61):12-29. doi: 10.1093/jncimonographs/lgad014. PMID: 37139973; PMCID: PMC10157791.

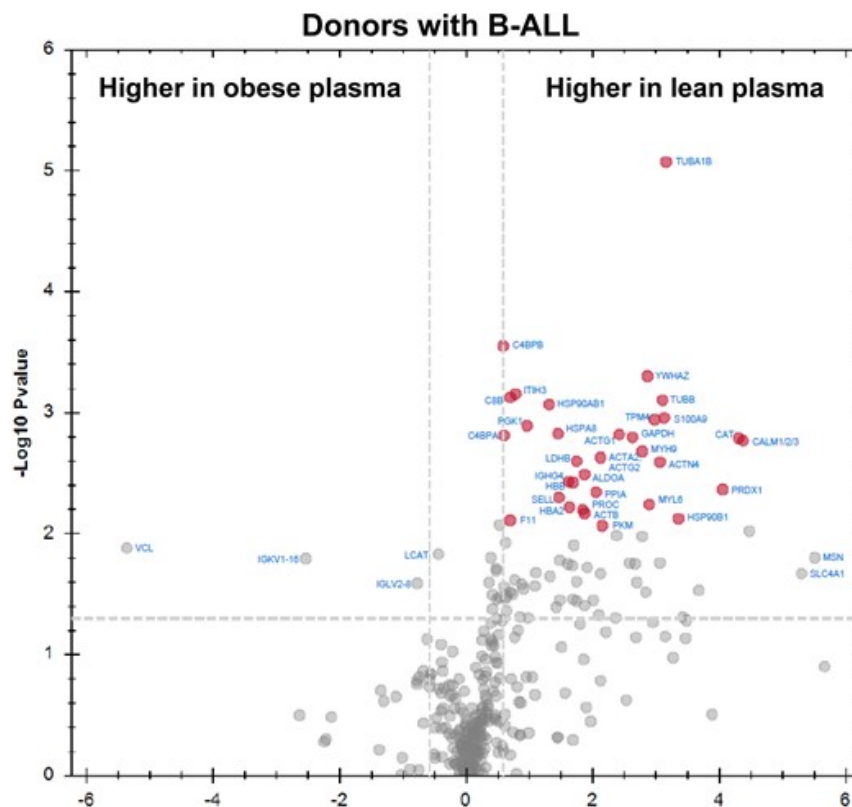


Figure 7: “The plasma of lean pediatric patients with B-ALL is exclusively characterized by the presence of heat shock proteins, cytoskeletal proteins, and proteins that promote cardiovascular health. The plasma of 14 pediatric patients with B-ALL (7 in the recommended body mass index range and 7 with obesity) was profiled using mass spectrometry. Proteins statistically significantly increased in healthy donors and those with obesity are indicated in red as determined by analysis using Spectronaut. B-ALL = B-cell acute lymphoblastic leukemia.”

Citation: Geitgey DK, Lee M, Cottrill KA, Jaffe M, Pilcher W, Bhasin S, Randall J, Ross AJ, Salemi M, Castillo-Castrejon M, Kilgore MB, Brown AC, Boss JM, Johnston R, Fitzpatrick AM, Kemp ML, English R, Weaver E, Bagchi P, Walsh R, Scharer CD, Bhasin M, Chandler JD, Haynes KA, Wellberg EA, Henry CJ. The 'omics of obesity in B-cell acute lymphoblastic leukemia. *J Natl Cancer Inst Monogr.* 2023 May 4;2023(61):12-29. doi: 10.1093/jncimonographs/lgad014. PMID: 37139973; PMCID: PMC10157791.

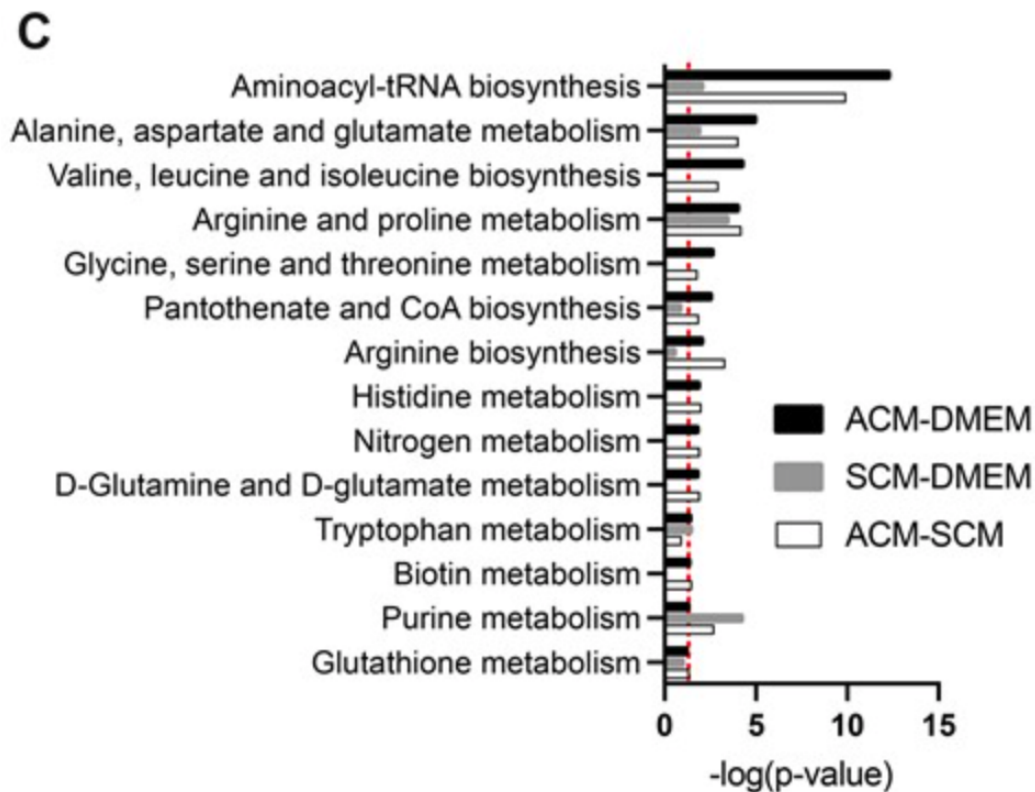


Figure 8: “Adipocytes secrete metabolites which may promote the growth of cancer cells.

C) Pathway enrichment analyses were performed by Metaboanalyst on metabolites identified by Tukey post hoc analysis to differ between ACM vs DMEM (**black**), SCM s DMEM (**grey**), and ACM vs SCM (**white**). Only pathways with any *P* value less than .05 were included.”

Citation: Geitgey DK, Lee M, Cottrill KA, Jaffe M, Pilcher W, Bhasin S, Randall J, Ross AJ, Salemi M, Castillo-Castrejon M, Kilgore MB, Brown AC, Boss JM, Johnston R, Fitzpatrick AM, Kemp ML, English R, Weaver E, Bagchi P, Walsh R, Scharer CD, Bhasin M, Chandler JD, Haynes KA, Wellberg EA, Henry CJ. The 'omics of obesity in B-cell acute lymphoblastic leukemia. *J Natl Cancer Inst Monogr.* 2023 May 4;2023(61):12-29. doi: 10.1093/jncimonographs/lgad014. PMID: 37139973; PMCID: PMC10157791.

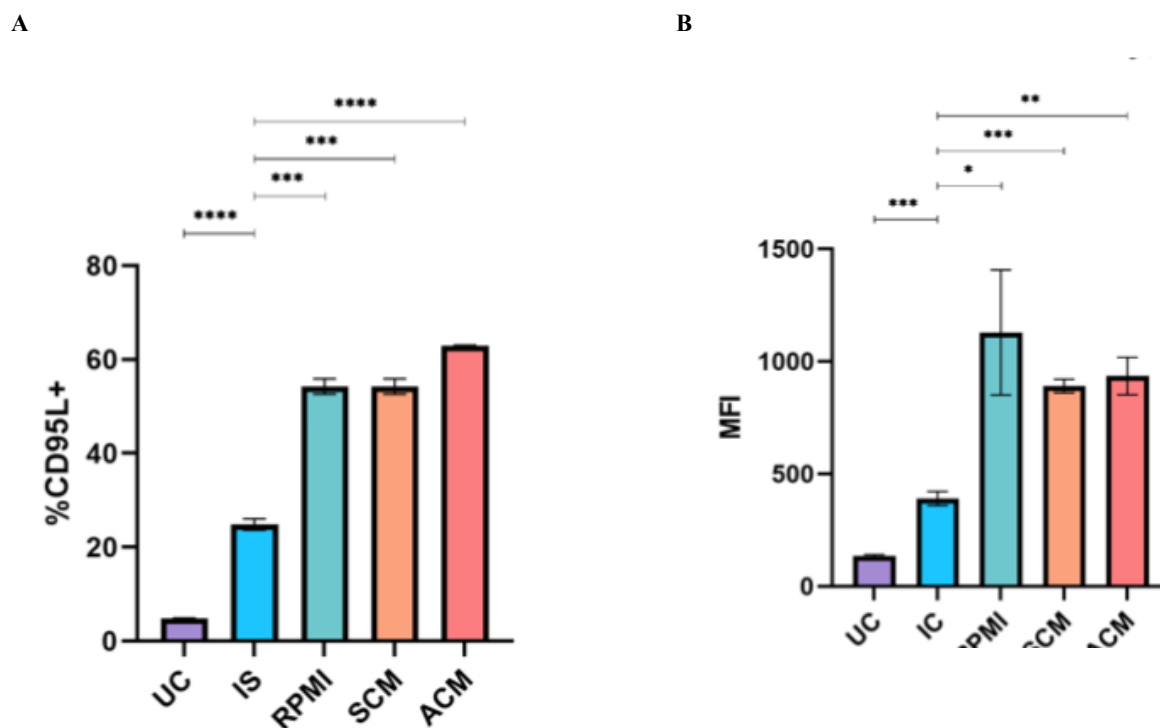


Figure 10: “CD19 and CD95L Surface Ligand is stably expressed at high levels on B-ALL Cells. A) Percent of B-ALL cells that express CD95L in Different Growth Conditions.

“CD95L expression in unstained control (UC), isotype control (IS), ACM, UCM, and SCM was measured by quantifying CD95L fluorescent antibody illuminance using flow cytometry. Means \pm s.d. are shown (** $p < 0.01$, ** $p < .01$, * $p < .05$ $n = 5$ independent experiments, unpaired t-test)”. **B) Mean Fluorescent Intensity of CD95L on B-ALL cells in Different Growth**

Conditions. CD95L fluorescence intensity was measured using CD95L antibodies and flow cytometry techniques. “Conditions are unstained control (UC), isotype control (IC), ACM, UCM, and SCM. Means \pm s.d. are shown (** $p < 0.01$, ** $p < .01$, * $p < .05$ $n = 5$ independent experiments, unpaired t-test).”

Citation:

Armah, K. (2022). *Hygiene Hypothesis in Acute Lymphoblastic Leukemia*. [Honors Thesis, Emory College].

<https://etd.library.emory.edu/concern/etds/g445cf47b?locale=en>

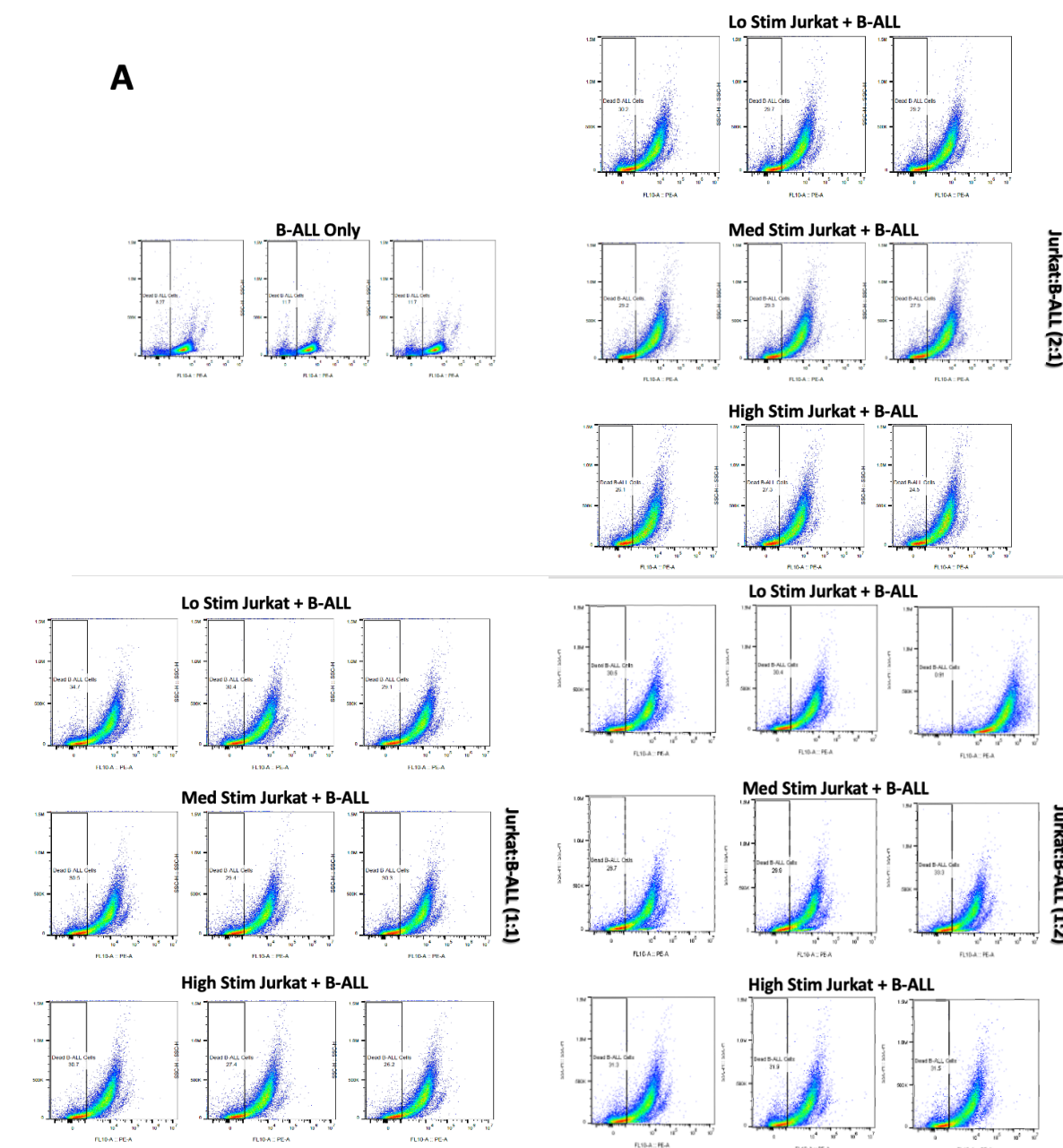


Figure 11: Jurkat T-Cells Recognize and Induce Apoptosis in Human B-ALL cells in a Non-Antigen Specific Manner Human B-ALL cells were plated at 5.0×10^4 cells/well in 96-well flat bottom plate with PMA/Ionomycin stimulated Jurkat T-cells were then added at 2:1 Jurkat T:B-ALL cells (10^5 cells/well); 1:1 Jurkat T:B-ALL cells (5.0×10^4 cells/well); 1:2 Jurkat T:B-ALL cells (2.5×10^4 cells/well).

SECTION V: REFERENCES

1. Juliusson, G., & Hough, R. (2016). Leukemia. *Progress in tumor research*, 43, 87–100.
<https://doi.org/10.1159/000447076>
2. Pierotti MA, Sozzi G, Croce CM. Discovery and identification of oncogenes. In: Kufe DW, Pollock RE, Weichselbaum RR, et al., editors. *Holland-Frei Cancer Medicine*. 6th edition. Hamilton (ON): BC Decker; 2003. Available from:
<https://www.ncbi.nlm.nih.gov/books/NBK13714/>
3. Hanahan D , Weinberg RA . The hallmarks of cancer. *Cell* 2000;100:57–70.
4. Hanahan D , Weinberg RA . Hallmarks of cancer: the next generation. *Cell* 2011;144:646–74.
5. Yang, D., Liu, J., Qian, H. *et al.* Cancer-associated fibroblasts: from basic science to anticancer therapy. *Exp Mol Med* 55, 1322–1332 (2023). <https://doi.org/10.1038/s12276-023-01013-0>
6. Melo JV (1997) BCR-ABL gene variants. *Baillière's Clinical Haematology* 10, 203–222.
7. Shady Adnan Awad, Helena Hohtari, Komal Kumar Javarappa, Tania Brandstoetter, Daehong Kim, Swapnil Potdar, Caroline A Heckman, Soili Kytölä, Kimmo Porkka, Eszter Doma, Veronika Sexl, Matti Kankainen, Satu Mustjoki; BCR-ABL1 p190 in CML: A Minor Breakpoint with a Major Impact. *Blood* 2019; 134 (Supplement_1): 190. doi: <https://doi.org/10.1182/blood-2019-126584>
8. Leak S, Horne GA and Copland M (2023). Targeting BCR-ABL1- positive leukaemias: a review article. *Cambridge Prisms: Precision Medicine*, 1, e21, 1–10
9. Lucas CM, Harris RJ, Giannoudis A, Knight K, Watmough SJ, Clark RE. BCR-ABL1 tyrosine kinase activity at diagnosis, as determined via the pCRKL/CRKL ratio, is

- predictive of clinical outcome in chronic myeloid leukaemia. *Br J Haematol.* 2010 May;149(3):458-60. doi: 10.1111/j.1365-2141.2009.08066.x. Epub 2010 Jan 11. PMID: 20067558.
10. Liam CCK, Boo YL, Chong SL, Sathar J, Ong TC, Tan SM. Philadelphia-positive (PH+) acute lymphoblastic leukemia (ALL): developing strategies for curing this stubborn disease. *Blood Res.* 2022 Jun 30;57(2):158-161. doi: 10.5045/br.2022.2020305. Epub 2022 May 30. PMID: 35620904; PMCID: PMC9242836.
 11. Cortes JE, Talpaz M, Kantarjian H. Chronic myelogenous leukemia: a review. *Am J Med.* 1996 May;100(5):555-70. doi: 10.1016/s0002-9343(96)00061-7. PMID: 8644769.
 12. Leak S, Horne GA and Copland M (2023). Targeting BCR-ABL1- positive leukaemias: a review article. *Cambridge Prisms: Precision Medicine*, 1, e21, 1–10
<https://doi.org/10.1017/pcm.2023.9>
 13. Vidal P. Interferon α in cancer immunoediting: From elimination to escape. *Scand J Immunol.* 2020;91:e12863. <https://doi.org/10.1111/sji.12863>
 14. SEER Cancer Stat Facts: Chronic Myeloid Leukemia. National Cancer Institute. Bethesda, MD, <https://seer.cancer.gov/statfacts/html/cm1l.html>
 15. Deininger M, Buchdunger E, Druker BJ. The development of imatinib as a therapeutic agent for chronic myeloid leukemia. *Blood.* 2005 Apr 1;105(7):2640-53. doi: 10.1182/blood-2004-08-3097. Epub 2004 Dec 23. PMID: 15618470.
 16. Druker BJ, Sawyers CL, Kantarjian H, Resta DJ, Reese SF, Ford JM, Capdeville R, Talpaz M. Activity of a specific inhibitor of the BCR-ABL tyrosine kinase in the blast crisis of chronic myeloid leukemia and acute lymphoblastic leukemia with the Philadelphia chromosome. *N Engl J Med.* 2001 Apr 5;344(14):1038-42. doi:

- 10.1056/NEJM200104053441402. Erratum in: N Engl J Med 2001 Jul 19;345(3):232.
PMID: 11287973.
17. Hochhaus A, Kantarjian H. The development of dasatinib as a treatment for chronic myeloid leukemia (CML): from initial studies to application in newly diagnosed patients. J Cancer Res Clin Oncol. 2013 Dec;139(12):1971-84. doi: 10.1007/s00432-013-1488-z. Epub 2013 Aug 13. PMID: 23942795; PMCID: PMC3825579.
18. Quintás-Cardama A, Cortes J. Molecular biology of bcr-abl1-positive chronic myeloid leukemia. Blood. 2009 Feb 19;113(8):1619-30. doi: 10.1182/blood-2008-03-144790. Epub 2008 Sep 30. PMID: 18827185; PMCID: PMC3952549.
19. Reddy EP, Aggarwal AK. The ins and outs of bcr-abl inhibition. Genes Cancer. 2012 May;3(5-6):447-54. doi: 10.1177/1947601912462126. PMID: 23226582; PMCID: PMC3513788.
20. Choi EJ. Asciminib: the first-in-class allosteric inhibitor of BCR::ABL1 kinase. Blood Res. 2023 Apr 30;58(S1):S29-S36. doi: 10.5045/br.2023.2023017. Epub 2023 Mar 9. PMID: 36891575; PMCID: PMC10133857.
21. Varadarajan, I., & Ballen, K. (2022). Advances in Cellular Therapy for T-Cell Prolymphocytic Leukemia. *Frontiers in oncology*, 12, 781479.
<https://doi.org/10.3389/fonc.2022.781479>
22. Suzuki R, Matsushita H, Kawai H, Matsuzawa H, Tsuboi K, Watanabe S, Kawada H, Ogawa Y, Ando K. Identification of a novel SEPT9-ABL1 fusion gene in a patient with T-cell prolymphocytic leukemia. Leuk Res Rep. 2014 Jun 28;3(2):54-7. doi: 10.1016/j.lrr.2014.06.004. PMID: 25068103; PMCID: PMC4110883.

23. Connolly D, Abdesselam I, Verdier-Pinard P, Montagna C. Septin roles in tumorigenesis. *Biol Chem*. 2011 Aug;392(8-9):725-38. doi: 10.1515/BC.2011.073. Epub 2011 Jul 11. PMID: 21740328.
24. Mangi MH, Newland AC. Interleukin-3: Promises and Perspectives. *Hematology*. 1998;3(1):55-66. doi: 10.1080/10245332.1998.11752123. PMID: 27416283.
25. Kawai, H., Matsushita, H., Suzuki, R., Sheng, Y., Lu, J., Matsuzawa, H., Yahata, T., Tsuma-Kaneko, M., Tsukamoto, H., Kawada, H., Ogawa, Y., & Ando, K. (2014). Functional analysis of the SEPT9-ABL1 chimeric fusion gene derived from T-prolymphocytic leukemia. *Leukemia Research*, 38(12), 1451-1459. <https://doi.org/10.1016/j.leukres.2014.08.015>
26. Colon Ramos A, Tarekegn K, Aujla A, Garcia de de Jesus K, Gupta S. T-Cell Prolymphocytic Leukemia: An Overview of Current and Future Approaches. *Cureus*. 2021 Feb 9;13(2):e13237. doi: 10.7759/cureus.13237. PMID: 33728186; PMCID: PMC7948687.
27. Geitgey DK, Lee M, Cottrill KA, Jaffe M, Pilcher W, Bhasin S, Randall J, Ross AJ, Salemi M, Castillo-Castrejon M, Kilgore MB, Brown AC, Boss JM, Johnston R, Fitzpatrick AM, Kemp ML, English R, Weaver E, Bagchi P, Walsh R, Scharer CD, Bhasin M, Chandler JD, Haynes KA, Wellberg EA, Henry CJ. The 'omics of obesity in B-cell acute lymphoblastic leukemia. *J Natl Cancer Inst Monogr*. 2023 May 4;2023(61):12-29. doi: 10.1093/jncimonographs/lgad014. PMID: 37139973; PMCID: PMC10157791.

28. Ward ZJ, Bleich SN, Cradock AL, et al. Projected U.S. state-level prevalence of adult obesity and severe obesity. *N Engl J Med.* 2019;381(25):2440-2450.
doi:10.1056/NEJMsa1909301.
29. Honce R, Schultz-Cherry S. Impact of obesity on influenza A virus pathogenesis, immune response, and evolution. *Front Immunol.* 2019;10:1071.
doi:10.3389/fimmu.2019.01071
30. Petrelli F, Cortellini A, Indini A, et al. Association of obesity with survival outcomes in patients with cancer: a systematic review and meta-analysis. *JAMA Netw Open.* 2021;4(3):e213520. doi:10.1001/jamanetworkopen.2021.3520
31. Sun W, Malvar J, Sposto R, Verma A, Wilkes JJ, Dennis R, Heym K, Laetsch TW, Widener M, Rheingold SR, Oesterheld J, Hijiya N, Sulis ML, Huynh V, Place AE, Bittencourt H, Hutchinson R, Messinger Y, Chang B, Matloub Y, Ziegler DS, Gardner R, Cooper T, Ceppi F, Hermiston M, Dalla-Pozza L, Schultz KR, Gaynon P, Wayne AS, Whitlock JA. Outcome of children with multiply relapsed B-cell acute lymphoblastic leukemia: a therapeutic advances in childhood leukemia & lymphoma study. *Leukemia.* 2018 Nov;32(11):2316-2325. doi: 10.1038/s41375-018-0094-0. Epub 2018 Mar 15.
PMID: 29728694; PMCID: PMC6224404.
32. Huang FL, Liao EC, Li CL, Yen CY, Yu SJ. Pathogenesis of pediatric B-cell acute lymphoblastic leukemia: Molecular pathways and disease treatments. *Oncol Lett.* 2020 Jul;20(1):448-454. doi: 10.3892/ol.2020.11583. Epub 2020 May 4. PMID: 32565969; PMCID: PMC7285861.

33. Anna Płotka, Krzysztof Lewandowski; *BCR/ABLI*-Like Acute Lymphoblastic Leukemia: From Diagnostic Approaches to Molecularly Targeted Therapy. *Acta Haematol* 23 March 2022; 145 (2): 122–131. <https://doi.org/10.1159/000519782>
34. Lee M, Hamilton JAG, Talekar GR, et al. Obesity-induced galectin- 9 is a therapeutic target in B-cell acute lymphoblastic leukemia. *Nat Commun.* 2022;13(1):1157. doi:10.1038/s41467-022-28839-y.
35. Sheng X, Tucci J, Parmentier JH, et al. Adipocytes cause leukemia cell resistance to daunorubicin via oxidative stress response. *Oncotarget.* 2016;7(45):73147-73159. doi:10.18632/onco-target.12246.
36. Wojtuszkiewicz A, Peters GJ, van Woerden NL, et al. Methotrexate resistance in relation to treatment outcome in childhood acute lymphoblastic leukemia. *J Hematol Oncol.* 2015; 8(1):61. doi:10.1186/s13045-015-0158-9.
37. Bertino JR. Karnofsky memorial lecture. Ode to methotrexate. *J Clin Oncol.* 1993;11(1):5-14. doi:10.1200/J Clin Oncol.1993.11.1.5.
38. Pogodziński D, Ostrowska L, Smarkusz-Zarzecka J, Zyśk B. Secretome of Adipose Tissue as the Key to Understanding the Endocrine Function of Adipose Tissue. *Int J Mol Sci.* 2022 Feb 19;23(4):2309. doi: 10.3390/ijms23042309. PMID: 35216423; PMCID: PMC8878787.
39. Tu H, McQuade JL, Davies MA, Huang M, Xie K, Ye Y, Chow WH, Rodriguez A, Wu X. Body mass index and survival after cancer diagnosis: A pan-cancer cohort study of 114 430 patients with cancer. *Innovation (Camb).* 2022 Oct 18;3(6):100344. doi: 10.1016/j.xinn.2022.100344. PMID: 36353671; PMCID: PMC9638833.

40. Pramanik R, Sheng X, Ichihara B, Heisterkamp N, Mittelman SD. Adipose tissue attracts and protects acute lymphoblastic leukemia cells from chemotherapy. *Leuk Res.* 2013 May;37(5):503-9. doi: 10.1016/j.leukres.2012.12.013. Epub 2013 Jan 17. PMID: 23332453; PMCID: PMC3622767.
41. Ehsanipour EA, Sheng X, Behan JW, et al. Adipocytes cause leukemia cell resistance to L-asparaginase via release of glutamine. *Cancer Res.* 2013;73(10):2998-3006. doi:10.1158/0008-5472.CAN-12-4402.
42. Behan JW, Yun JP, Proektor MP, et al. Adipocytes impair leukemia treatment in mice. *Cancer Res.* 2009;69(19):7867-7874. doi: 10.1158/0008-5472.CAN-09-0800.
43. Tucci J, Chen T, Margulis K, et al. Adipocytes provide fatty acids to acute lymphoblastic leukemia cells. *Front Oncol.* 2021;11: 665763. doi:10.3389/fonc.2021.665763.
44. Sheng X, Tucci J, Parmentier JH, et al. Adipocytes cause leukemia cell resistance to daunorubicin via oxidative stress response. *Oncotarget.* 2016;7(45):73147-73159. doi:10.18632/oncotarget.12246.
45. Wang Z, Liu F, Fan N, et al. Targeting glutaminolysis: new perspectives to understand cancer development and novel strategies for potential target therapies. *Front Oncol.* 2020;10: 589508. doi:10.3389/fonc.2020.589508.
46. Jiang XC, Yu Y. The role of phospholipid transfer protein in the development of atherosclerosis. *Curr Atheroscler Rep.* 2021; 23(3):9. doi:10.1007/s11883-021-00907-6.
47. Jiang XC. Phospholipid transfer protein: its impact on lipoprotein homeostasis and atherosclerosis. *J Lipid Res.* 2018;59(5): 764-771. doi:10.1194/jlr.R082503.

48. Sanjurjo L, Aran G, Roher N, Valledor AF, Sarrias MR. AIM/ CD5L: a key protein in the control of immune homeostasis and inflammatory disease. *J Leukoc Biol.* 2015;98(2):173-184. doi: 10.1189/jlb.3RU0215-074R.
49. Sahu N, Dela Cruz D, Gao M, et al. Proline starvation induces unresolved ER stress and hinders mTORC1-dependent tumorigenesis. *Cell Metab.* 2016;24(5):753-761. doi:10.1016/j.cmet.2016.08.008.
50. Garcia-Bermudez J, Baudrier L, La K, et al. Aspartate is a limiting metabolite for cancer cell proliferation under hypoxia and in tumours. *Nat Cell Biol.* 2018;20(7):775-781. doi:10.1038/s41556-018-0118-z.
51. Chen YC, Navarrete MS, Wang Y, et al. N-myristoyltransferase-1 is necessary for lysosomal degradation and mTORC1 activation in cancer cells. *Sci Rep.* 2020;10(1):11952. doi: 10.1038/s41598-020-68615-w.
52. Lempesis IG, van Meijel RLJ, Manolopoulos KN, Goossens GH. Oxygenation of adipose tissue: A human perspective. *Acta Physiol (Oxf).* 2020 Jan;228(1):e13298. doi: 10.1111/apha.13298. Epub 2019 Jun 2. PMID: 31077538; PMCID: PMC6916558.
53. AntRoss, Miyoung Lee, Jamie Hamilton, Raira Ank, Priscilla Do, Jamie Story, Sunil S. Raikar, Erik Dreaden, Christopher C. Porter, Curtis J. Henry. Obesity Attenuates T-Cell Function Which Impacts the Efficacy of T-Cell Based Immunotherapies in Acute Lymphoblastic Leukemia, *Blood*, Volume 136, Supplement 1, 2020, Pages 25-26, ISSN 0006-4971, <https://doi.org/10.1182/blood-2020-136573>.
54. Frasca D, Romero M, Garcia D, Diaz A, Blomberg BB. Obesity accelerates age-associated defects in human B cells through a metabolic reprogramming induced by the fatty acid palmitate. *Front Aging.* 2021;2:828697. doi:10.3389/fragi.2021.828697.

55. Christian R. Schultze-Florey, Christophe Peczynski, William Boreland, Michael Daskalakis, Anne Sirvent, Ibrahim Yakoub-Agha, Maria-Luisa Schubert, Christof Scheid, Anne Huynh, Victoria Potter, Didier Blaise, Matthew P. Collin, Rafael Hernani, Gerald G. Wulf, Francis A. Ayuk, Caroline Besley, Lucia Lopez Corral, Edouard Forcade, Peter Vandenberghe, Dominik Schneidawind, Matthias Stelljes, Friedrich Stölzel, Bertram Glass, Ivan Sergeevich Moiseev, Helene Schoemans, Olaf Penack, Christian Koenecke, Zinaida Peric; High Body Mass Index Is Associated with Favorable Outcome in Younger Patients Receiving CD19 CAR T-Cell Therapy for B-Cell Lymphoma: A Retrospective Study from the EBMT Transplant Complications Working Party. *Blood* 2023; 142 (Supplement 1): 4867.
doi: <https://doi.org/10.1182/blood-2023-187393>
56. Molina O, Ortega-Sabater C, Thampi N, Fernández-Fuentes N, Guerrero-Murillo M, Martínez-Moreno A, Vinyoles M, Velasco-Hernández T, Bueno C, Trincado JL, Granada I, Campos D, Giménez C, Boer JM, den Boer ML, Calvo GF, Camós M, Fuster JL, Velasco P, Ballerini P, Locatelli F, Mullighan CG, Spierings DCJ, Foijer F, Pérez-García VM, Menéndez P. Chromosomal instability in aneuploid acute lymphoblastic leukemia associates with disease progression. *EMBO Mol Med*. 2024 Jan;16(1):64-92. doi: 10.1038/s44321-023-00006-w. Epub 2023 Dec 15. PMID: 38177531; PMCID: PMC10897411.
57. Kim SK, Cho SW. The Evasion Mechanisms of Cancer Immunity and Drug Intervention in the Tumor Microenvironment. *Front Pharmacol*. 2022 May 24;13:868695. doi: 10.3389/fphar.2022.868695. PMID: 35685630; PMCID: PMC9171538.

58. Masschelin PM, Cox AR, Chernis N, Hartig SM. The Impact of Oxidative Stress on Adipose Tissue Energy Balance. *Front Physiol.* 2020 Jan 22;10:1638. doi: 10.3389/fphys.2019.01638. PMID: 32038305; PMCID: PMC6987041.
59. Perkin MR, Strachan DP. The hygiene hypothesis for allergy - conception and evolution. *Front Allergy.* 2022 Nov 24;3:1051368. doi: 10.3389/falgy.2022.1051368. PMID: 36506644; PMCID: PMC9731379.
60. Urayama KY, Ma X, Selvin S, Metayer C, Chokkalingam AP, Wiemels JL, Does M, Chang J, Wong A, Trachtenberg E, Buffler PA. Early life exposure to infections and risk of childhood acute lymphoblastic leukemia. *Int J Cancer.* 2011 Apr 1;128(7):1632-43. doi: 10.1002/ijc.25752. Epub 2010 Dec 17. PMID: 21280034; PMCID: PMC3165002.
61. Peter, M., Hadji, A., Murmann, A. *et al.* The role of CD95 and CD95 ligand in cancer. *Cell Death Differ* **22**, 549–559 (2015). <https://doi.org/10.1038/cdd.2015.3>
62. Shah, N.N., Johnson, B.D., Schneider, D. et al. Bispecific anti-CD20, anti-CD19 CAR T cells for relapsed B cell malignancies: a phase 1 dose escalation and expansion trial. *Nat Med* 26, 1569–1575 (2020). <https://doi.org/10.1038/s41591-020-1081-3>
63. Philipp N, Kazerani M, Nicholls A, Vick B, Wulf J, Straub T, Scheurer M, Muth A, Hänel G, Nixdorf D, Sponheimer M, Ohlmeyer M, Lacher SM, Brauchle B, Marcinek A, Rohrbacher L, Leutbecher A, Rejeski K, Weigert O, von Bergwelt-Baildon M, Theurich S, Kischel R, Jeremias I, Bücklein V, Subklewe M. T-cell exhaustion induced by continuous bispecific molecule exposure is ameliorated by treatment-free intervals. *Blood.* 2022 Sep 8;140(10):1104-1118. doi: 10.1182/blood.2022015956. PMID: 35878001; PMCID: PMC10652962.

64. Lee J, Ahn E, Kissick HT, Ahmed R. Reinvigorating Exhausted T Cells by Blockade of the PD-1 Pathway. *For Immunopathol Dis Therap*. 2015;6(1-2):7-17. doi: 10.1615/ForumImmunDisTher.2015014188. PMID: 28286692; PMCID: PMC5341794.
65. O'Connell P, Hyslop S, Blake MK, Godbehere S, Amalfitano A, Aldhamen YA. SLAMF7 Signaling Reprograms T Cells toward Exhaustion in the Tumor Microenvironment. *J Immunol*. 2021 Jan 1;206(1):193-205. doi: 10.4049/jimmunol.2000300. Epub 2020 Dec 7. PMID: 33288545; PMCID: PMC7855551.
66. Hochhaus A, Réa D, Boquimpani C, Minami Y, Cortes JE, Hughes TP, Apperley JF, Lomaia E, Voloshin S, Turkina A, Kim DW, Abdo A, Fogliatto LM, le Coutre P, Sasaki K, Kim DDH, Saussele S, Annunziata M, Chaudhri N, Chee L, García-Gutiérrez V, Kapoor S, Allepuz A, Quenet S, Bédoucha V, Mauro MJ. Asciminib vs bosutinib in chronic-phase chronic myeloid leukemia previously treated with at least two tyrosine kinase inhibitors: longer-term follow-up of ASCSEMBL. *Leukemia*. 2023 Mar;37(3):617-626. doi: 10.1038/s41375-023-01829-9. Epub 2023 Jan 30. PMID: 36717654; PMCID: PMC9991909.
67. Armah, K. (2022). *Hygiene Hypothesis in Acute Lymphoblastic Leukemia*. [Honors Thesis, Emory College]. <https://etd.library.emory.edu/concern/etds/g445cf47b?locale=en>